Optik 126 (2015) 5109–5114

Contents lists available at ScienceDirect

Optik

journal homepage: www.elsevier.de/ijleo

Analytical investigations of CdS nanostructures for optoelectronic applications

Y. Al-Douri [a,d,*], A.H. Reshak [b,c]

[a] Institute of Nano Electronic Engineering, University Malaysia Perlis, 01000 Kangar, Perlis, Malaysia
[b] New Technologies – Research Center, University of West Bohemia, Univerzitni 8, 306 14 Pilsen, Czech Republic
[c] Center of Excellence Geopolymer and Green Technology, School of Material Engineering, University Malaysia Perlis, 01007 Kangar, Perlis, Malaysia
[d] Physics Department, Faculty of Science, University of Sidi-Bel-Abbes, 22000, Algeria

ARTICLE INFO

Article history:
Received 17 November 2014
Accepted 25 September 2015

Keywords:
CdS nanostructure
Particle size
Optical properties

ABSTRACT

Cadmium sulfide (CdS) nanostructures were prepared and deposited on glass substrates of Cd:S (1.2–0.05 mol/L) annealed at 400 °C with different spin coating speed (1000, 3000 and 5000 rpm) using spin coating technique. Structural, morphological and analytical studies were investigated by X-ray diffraction (XRD), atomic force microscopy (AFM), Fourier transform infrared (FTIR) and UV–Vis Spectroscopy. It is found that the particle size of CdS nanostructures is 1.40, 1.78 and 2.31 nm prepared at 1000, 3000 and 5000 rpm, respectively. The band gap was measured with an indication of transmission within the visible range; it is changed due to particle size of CdS nanostructures. The calculated refractive index and optical dielectric constant results give agreement with experimental results. The obtained results are in accordance with experimental and theoretical data.

© 2015 Elsevier GmbH. All rights reserved.

1. Introduction

CdS nanostructures have attracted great interest in the recent years due to their unique chemical, physical, optical, electrical and transport properties [1,2]. Due to vast surface area, all nanostructured materials posses a high surface energy and thus, are thermodynamically unstable or metastable. One of the great challenges in fabrication and processing of nanomaterial is to overcome the surface energy and to prevent the nanomaterial from growth in size driven by the reduction of overall surface energy. Because of high surface energy of nanoparticles, they are extremely reactive and most systems without protection or passivation of their surfaces undergo aggregation [3]. Organic stabilizers are usually used to prevent nanoparticles from aggregation by capping their surfaces [4]. As the semiconductor nanoparticles exhibit size dependent properties, the melting point of CdS crystallites is as low as ~400 °C and the band gap of 0.7 nm CdS crystallite is 3.85 eV [5]. While at very high pressure, the phase changes from wurtzite to rock salt phase [6]. Since CdS has 2.43 eV (513 nm) band gap, so it is most promising candidate among II–VI compounds for detecting visible radiation. As CdS has wide band gap, it is used as window material for heterojunction solar cells to avoid the recombination of photogenerated carriers which improve the solar cells efficiency. It has also applied in light emitting diodes, photo detectors, sensors, address decoders and electrically driven lasers [7].

Al-Douri et al. [8] have used the density functional theory (DFT) for energy band calculations of CdS and CdTe to research the energetic transition and optical properties calculations as a function of quantum dot diameter. Also, they [9] have investigated the quantum dot potential using the full potential-linearized augmented plane wave (FP-LAPW) method, the energetic transition and optical properties calculations of Si. The refractive index and transverse effective charge are predicted as a function of dot diameter. Joshi et al. [10] have reported on growth of stoichiometric and nonstoichiometric nanostructured heterojunction solar cell of CdS/CuInS$_x$/Se$_{2-x}$ varying x from 0 to 2 in the interval of 0.5 using cost effective, simple, chemical ion exchange method at room temperature on ITO glass substrate. They have elaborated structural, compositional, optical and illumination studies, and have achieved the solar energy conversion efficiency which corresponds for stoichiometric dependent electron–hole pair generation and separation phenomenon. Finally, Böer [11] has enhanced the solar conversion efficiency of CdS/CdTe solar cells from 8 to 15% using thin layer of CdS of about 200 Å. The reason for this efficiency enhancement is typical for CdS. Also, he has summarized the technical and economical importance of these solar cells on the energy conversion market.

* Corresponding author. Tel.: +60 4 9798408; fax: +60 4 9798305.
E-mail address: yaldouri@yahoo.com (Y. Al-Douri).

http://dx.doi.org/10.1016/j.ijleo.2015.09.233
0030-4026/© 2015 Elsevier GmbH. All rights reserved.

In this work, detailed studies of structural and optical properties of CdS nanostructures deposited on glass substrates with different spin coating speeds at room temperature are reported. The organization of the paper is as follows: A description of the experimental procedure is given in Section 2. Section 3 presents the results and discussion concerning the structural and optical properties. The conclusion is given in Section 4.

2. Experimental process

All chemicals were of analytical grade were received from Malaysia Sigma–Aldrich company. CdS nanostructures were grown by sol–gel spin coating method at room temperature. Polyethylene glycol 200 (PEG) solvent was prepared by mixing 0.6 ml of PEG, 8.5 ml of ethanol and 0.5 ml of acetic acid under stirring for 1 h. 0.05 mol/L thiourea and 1.2 mol/L cadmium nitrate as a source of S and Cd, in addition to 15 ml ethanol accompanying 60 °C. Prepared solution was slowly added to PEG sol with vigorous stirring for 6 h. As the reaction was started, the reaction system gradually changed from transparent to light yellow. The precipitate collected from centrifugation was deposited on glass substrates that was dried at 120 °C on hot plate and annealed at 400 °C by furnace for 1 h. The samples were taken out after the furnace cooled down to room temperature. They are used to be analyzed and characterized by X-ray diffraction (XRD) pattern (Philips PW 1710 X-ray diffractometer), atomic force microscopy (AFM) (SII Sciko Instrument INC SPI 3800N Probe station), Fourier transform infrared spectroscopy (FTIR) and UV–Vis spectroscopy (Perkin Elmer Lambda 950), respectively.

3. Results and discussion

3.1. Structural properties

The structural properties of CdS nanostructures have been investigated by X-ray diffraction (XRD) technique as shown in Fig. 1, prepared by different spin coating speeds at 1000, 3000 and 5000 rpm and annealed for 1 h at 400 °C. XRD pattern has provided information about crystalline phase of nanoparticles as well as crystallite size. Fig. 1a shows the synthesized CdS nanoparticles. The peak is observed at 29.52° corresponding to (0 0 2) plane of hexagonal phase of CdS nanostructure prepared at 1000 rpm, while Fig. 1b shows CdS nanostructure prepared at 3000 rpm that appeared one peak at 25° corresponding to the (1 1 1) plane. Fig. 1c shows CdS nanostructure prepared at 5000 rpm that appeared one peak at 29.52° corresponding to (0 0 2) plane of hexagonal phase. The intensity of the peak is observed at CdS nanostructures deposited at 5000 rpm is higher than nanostructured CdS deposited at 1000 and 3000 rpm. This is an indication of good crystalline nature.

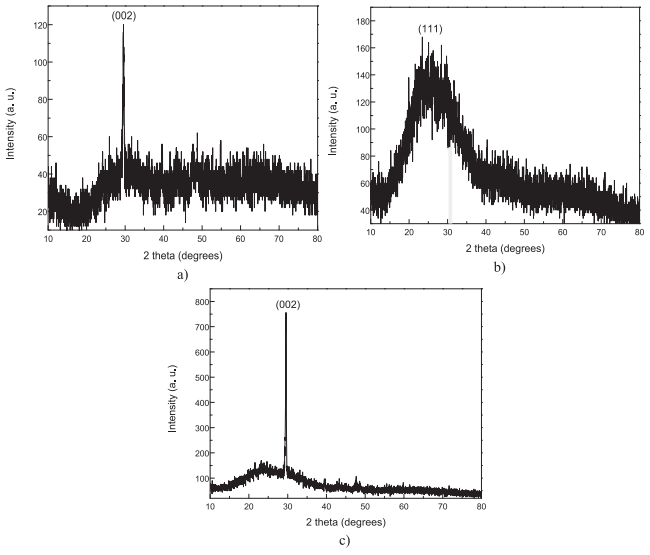

Fig. 1. X-ray diffraction (XRD) patterns of CdS nanostructures deposited on glass substrates, annealed at 400 °C: (a) 1000, (b) 3000 and (c) 5000 rpm spin coating speeds.

Crystallite size was calculated using Scherrer's formula [12]:

$$D = \frac{0.91\lambda}{\beta \cos\theta} \tag{1}$$

where D is the crystallite size, XRD patterns of the as synthesized sample was recorded on XRD using rotating anode with Cu-Kα line ($\lambda = 1.54$ Å), θ is the angle between the incident beam and the reflection lattice planes and β is the full width at half maxima (FWHM) of the diffraction peak in radian. Operating is at 35.0 kV, current = 25.0 mA, scan range = 10,000–80,000, scan speed = 5000 °/min and present time = 0.24 s. The particle size is increased with increasing the spin coating speed due to increasing lattice constants. In addition, the dislocation density (δ) and strain of CdS nanostructures (ε) were determined via XRD using the following relations [12]:

$$\delta = 1/D_{hkl}^2 \tag{2}$$

$$\varepsilon = \frac{\beta \cos\theta}{4} \tag{3}$$

The defects like dislocation density and strain in the CdS nanostructures are determined as given in Table 1, the highest dislocation density and the highest strain are found to be 3156.167×10^{14} lines/m^2 and 4.1237×10^{-3}, respectively of CdS nanostructures deposited at 3000 rpm, the interplanar distance (d) is calculated using Bragg's formula [12]:

$$d = \frac{n\lambda}{2 \sin\theta} \tag{4}$$

where n is constant equals 1. The interplanar distance (d) is found to be 1.54, 1.82 and 1.54 Å, respectively and the lattice constants a and c were calculated using Eqs. (5) and (6). The lattice constants are found to be $a = 1.026$, $c = 3.086$ Å, $a = 1.22$, $c = 3.65$ Å and $a = 1.30$, $c = 3.086$ Å for spin coating speeds 1000, 3000 and 5000 rpm, respectively.

$$a = \frac{\sqrt{1/3}\lambda}{\sin\theta} \tag{5}$$

$$c = \frac{\lambda}{\sin\theta} \tag{6}$$

The number of crystallites per unit area (N) is calculated using the following relation [12]:

$$N = \frac{t}{D^3} \tag{7}$$

where t is the thickness of nanostructured CdS as given by AFM. The number of crystallites is found to be 21.9, 0.71 and 0.82 grains/area for 1000, 3000 and 5000 rpm, respectively.

The bulk modulus is a reflectance of the materials stiffness that it is important in different industries. Many authors [13–18] have made various efforts to explore thermodynamic properties of solids. In these studies, authors have examined the thermodynamic properties such as the inter-atomic separation and the bulk modulus of solids with different approximations and best-fit relations [15–18]. It has become possible to compute with great accuracy an important number of structural and electronic properties of solids. The ab initio calculations are complex and require significant effort. Therefore, more empirical approaches have been developed [19,20] to compute properties of materials. In many cases, the empirical

Table 1
The measured structural properties using XRD data [25] correspond to the calculated B_o of CdS nanostructures..

Spin coating speed (rpm)/(s)	Peak[a] (θ)	Particle size[a] (nm)	Dislocaction density[a] (δ) (10^{14} lines/m^2)	Strain[a] (10^{-3})	Interplanar distance[a] (d) (Å)	Miller indices (hkl)	Lattice parametes[a] (Å)	No. crystallits[a] grains/area N ($\times 10^{15}$)	Bulk modulus[b] B_o (GPa)
1000/30	29.52	1.40	0.2381	0.2425	1.54	0 0 2	$a = 1.026$ $a = 4.086$[c] $a = 4.1$[d] $c = 3.086$ $c = 6.667$[c] $c = 6.7$[d]	21.9	54.23 69[e] 62[f] 66.6[g]
3000/30	25	1.78	3156.167	4.1237	1.82	1 1 1	$a = 1.22$ $c = 3.65$	7.1	30.14
5000/30	29.98	2.31	0.2162	0.1472	1.54	0 0 2	$a = 1.300$ $c = 3.750$	8.2	27.41

[a] Measured value.
[b] Calculated value.
[c] Ref. [13] Theo.
[d] Ref. [24] Exp.
[e] Ref. [21] cal.
[f] Ref. [22] Exp.
[g] Ref. [23] cal.

methods offer the advantage of applicability to broad class of materials and to illustrate trends. In many applications, these empirical approaches do not give highly accurate results for each specific material, but are still very useful. Cohen [21] has established an empirical formula for calculation of the bulk modulus B_o; based on the nearest-neighbor distance. His result is in agreement with experimental values. Lam et al. [22] have derived an analytical expression for the bulk modulus from the total energy. This expression is different in structure from the empirical formula but gives similar numerical results. Also, they have obtained an analytical expression for the pressure derivative B_o of the bulk modulus. Our group [23] used concept based on the lattice constant to establish empirical formula for the calculation of the bulk modulus. The calculated results are in agreement with experimental data and other calculations. Consideration of hypothetical structure and simulation of the experimental conditions are required to make practical use of this formula.

The aim is to see how qualitative concept, such as the bulk modulus, can be related to lattice constant. It was argued that the dominant effect is the degree of covalence characterized by Phillips' homopolar gap E_h [19], and one reason for presenting these data in this work is that the validity of our calculations that is not restricted in computed space. We thus believe that the data will prove valuable for future work in this field. An important reason for studying B_o is the observation of clear differences between the lattice constant for different CdS nanostructures. While the basis of our model is the lattice constant as seen in Table 1. Fitting of these data gives the following empirical formula [23]:

$$B_o = [3000 - 100\lambda]\left(\frac{a}{2}\right)^{-3.5} \quad (8)$$

where a is the lattice constant (in Å) and λ is empirical parameter which accounts for the effect of ionicity; $\lambda = 2$ for II–VI semiconductors. In Table 1, the calculated bulk modulus value is compared with experimental and theoretical [21–23] results. We may conclude that the calculated bulk moduli of CdS nanostructures are in accordance with other results [21–23] and exhibit the same trends as those found for the values derived from the experimental [22] value as seen in Table 1. Our results show that CdS nanostructure of the lowest speed is the hardest than other CdS nanostructures.

The CdS nanostructures are very helpful to study the surface topography of CdS nanostructures. The CdS nanostructures are well covered due to growth mechanism, although the distribution of the well-defined grains is not uniformed, but some enhancement of

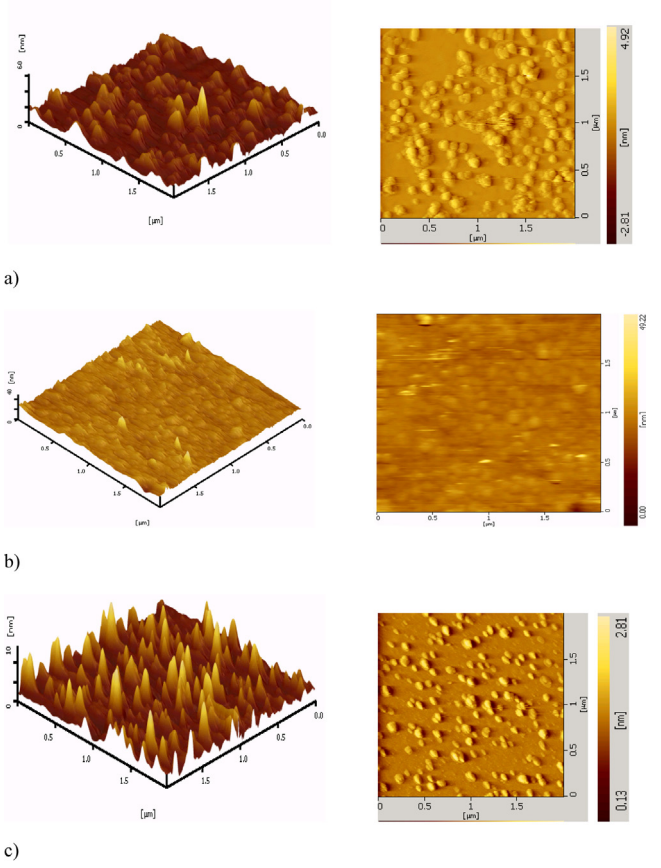

Fig. 2. Atomic force microscopy (AFM) images of CdS nanostructures deposited on glass substrates, annealed at 400 °C: (a) 1000, (b) 300 and (c) 5000 rpm spin coating speeds.

the structures is shown. Earlier workers [26–28] have found well developed structures, where they interpreted in terms of overlapping of different layers formed under continuous growth. Fig. 2 shows typical 2D and 3D dimension images using AFM, scan area 2000 nm (2 μm × 2 μm) and scan speed 2 Hz. The thickness of CdS nanostructures is shown in Fig. 2 and measured to be 60, 40 and 10 nm for 1000, 3000 and 5000 rpm, respectively. Castro-Rodriguez et al. [27] have demonstrated that the conversion efficiency of CdS solar cells strongly depends on the small roughness of CdS surface;

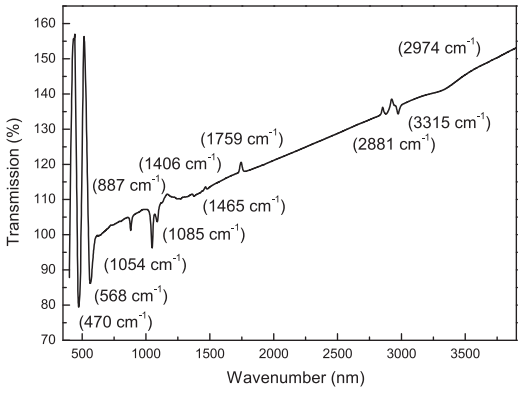

Fig. 3. Fourier transform infrared (FTIR) spectrum of CdS nanostructures at concentration of thiourea 0.05 mol/L on solvent.

a reduction of surface roughness tends to increase the conversion efficiency. However, as the rotation speed increases, the conversion efficiency of solar cells increases due to the surface thickness decreasing [28].

FTIR measurement has been made in the wave number range 400–4000 cm^{-1}. The FTIR spectrum and the corresponding data have been observed. Analysis of FTIR spectrum of CdS nanostructure was obtained. Fig. 3 shows weak absorption band present at 3315 cm^{-1} that is due to OH stretching vibration of water molecules and presence of moisture in the solution. It is shown two stretching bands, asymmetric and symmetric around 2974 and 2881 cm^{-1} that are associated with C—H stretching. The band at 1759 cm^{-1} is resulted from aromatic C—C stretching. Very weak bending vibrations of water molecules appeared at 1465 and 1406 cm^{-1} of C—C stretching. Medium strong band positions in the range of 1085, 1054 and 887 cm^{-1} are possibly due to stretching vibrations of sulfate group. The strong absorption band at 470 and 568 cm^{-1} corresponds to Cd—S stretching [29], translated into transition exceeded 100% and coincided with CdS energy gap equals 513 nm.

3.2. Optical properties

The optical properties are important to understand the behavior of semiconductor nanocrystals. A fundamental property of semiconductors is energy band gap separation between filled valence band and the empty conduction band. Optical excitations of electrons across the band gap are strongly allowed, producing an abrupt increase in absorption at the wavelength corresponding to the energy band gap. Fig. 4 shows the transmittance spectra in the wavelength range 250–800 nm of CdS nanostructures. It is around 85.40%, 87.49% and 85.70% transmission for CdS nanostructures prepared at 1000, 3000 and 5000 rpm, respectively. However, the prepared CdS nanostructure at 3000 rpm appears more than 87% transmission for wavelengths longer than 450 nm [30].

The optical band gap (E_g) of CdS nanostructures is determined as given in Table 2 by applying the Tauc's model [31], which allows one to directly estimate the E_g from the relation $(\alpha h\nu)^{1/n} = A(h\nu - E_g)$, where A is constant, α is the absorption coefficient = $0.023/d \times \mathrm{Ln}\,1/\mathrm{T}$, $h\nu$ is the photon energy, and n equals 1/2 for direct allowed transitions. Fig. 5 shows the relationship between $(\alpha h\nu)^2$ and $h\nu$. The E_g can be obtained by extrapolating the linear portion to the photon energy axis as shown in Fig. 5 [32].

The refractive index n_o is an important physical parameter related to microscopic atomic interactions. Theoretically, the two different approaches in viewing this subject are the refractive index related to density and the local polarizability of these entities [33]. On the other hand, the crystalline structure represented by delocalized picture, n_o will be closely related to the energy band structure of the material, complicated quantum mechanical analysis

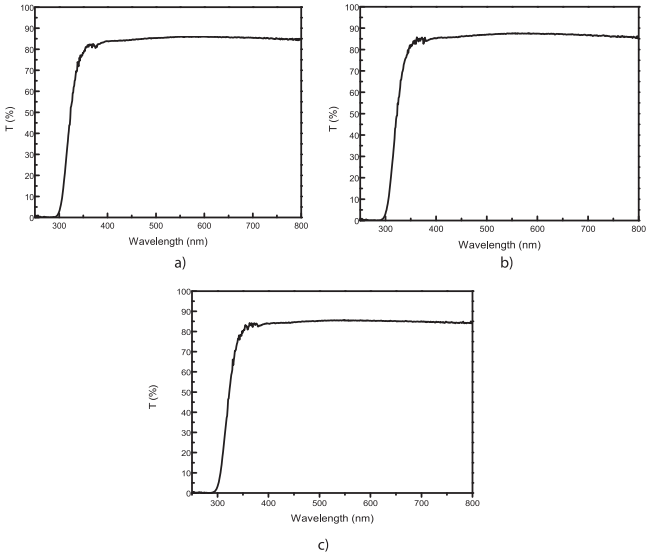

Fig. 4. Transmission spectra of CdS nanostructures deposited on glass substrates at (a) 1000, (b) 3000 and (c) 5000 rpm spin coating speeds.

Table 2
The measured transmission, thickness and energy gap (E_g) correspond to calculated refractive index (n_o) and optical dielectric constant (ε_∞) of CdS nanostructures using Ravindra et al. [36], Herve and Vandamme [37] and Ghosh et al. [38] models.

Transmission[a] (%)	Thickness[a] (nm)	Spin coating speed[a] (rpm)	E_g[a] (eV)	Refractive index (n_o)	Optical dielectric constant (ε_∞)
80–85	60	1000	2.00	5.2880[e]	27.9629[e]
			2.359[b]	2.7097[f]	7.3424[f]
			2.43[c]	5.8891[g]	34.6814[g]
			2.50[d]	2.529[h]	
82–85	40	3000	2.20	5.4120[e]	29.2897[e]
			2.359[b]	2.6263[f]	6.8974[f]
			2.43[c]	5.5886[g]	31.2324[g]
			2.50[d]	2.529[h]	
84–87	10	5000	2.15	5.3810[e]	28.9551[e]
			2.359[b]	2.6466[f]	7.0044[f]
			2.43[c]	5.7110[g]	32.6155[g]
			2.50[d]	2.529[h]	

[a] Measured value.
[b] Ref. [8] Theo.
[c] Ref. [32] Exp.
[d] Ref. [35] Exp.
[e] Ref. [36].
[f] Ref. [37].
[g] Ref. [38].
[h] Ref. [35] Exp.

requirements and the obtained results. Many attempts have been made to relate the refractive index and the energy gap E_g through simple relationships [34,35]. Here, the various relationships between n_o and E_g will be reviewed. Ravindra et al. [36] have suggested different relationships between the band gap and the high frequency refractive index and presented linear form of n_o as a function of E_g:

$$n_o = \alpha + \beta E_g \tag{9}$$

where $\alpha = 4.048$ and $\beta = -0.62\ \mathrm{eV}^{-1}$.

To be inspired by simple physics of light refraction and dispersion, Herve and Vandamme have [37] proposed an empirical relation as:

$$n_o = \sqrt{1 + \left(\frac{A}{E_g + B}\right)^2}, \tag{10}$$

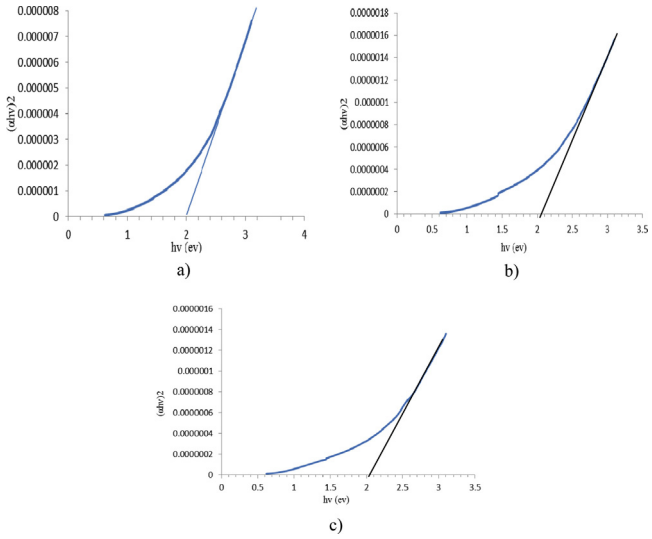

Fig. 5. $(\alpha h\nu)^2$ versus $h\nu$ dependency of CdS nanostructures deposited on glass substrates, annealed at 400 °C for 1 h: (a) 1000, (b) 3000 and (c) 5000 rpm spin coating speeds.

where $A = 13.6$ eV and $B = 3.4$ eV. Ghosh et al. [38] have took different approach to the problem by considering the band structural and quantum-dielectric formulations of Penn [39] and Van Vechten [40]. Introducing A as the contribution from the valence electrons and B as a constant additive to the lowest band gap E_g, the expression for the high-frequency refractive index is written as:

$$n_o^2 - 1 = \frac{A}{(E_g + B)^2}, \tag{11}$$

where $A = 25E_g + 212$, $B = 0.21E_g + 4.25$ and $(E_g + B)$ refers to an appropriate average energy gap of the material. Thus, these three models of variation n_o with energy gap have been calculated. Also, the calculated values of optical dielectric constant (ε_∞) were obtained using the relation $\varepsilon_\infty = {n_o}^2$ [41]. Our calculated refractive index values are in agreement with experimental value [35] as given in Table 2. This is giving an appropriate model of Herve and Vandamme for photovoltaic and optoelectronic applications.

4. Conclusion

Spin coating technique has been successfully developed to synthesize CdS nanostructures. XRD patterns showed diffraction lines of CdS nanostructures that have hexagonal structure. The particle size increases as the spin coating speed increases. The thickness decreases as the spin coating speed increases. UV–Vis spectroscopy shows higher transmission at 3000 rpm. The band gap of CdS nanostructures varies between 2.00, 2.20 and 2.15 eV for different spin coating speeds. The refractive index is proven that Herve and Vandamme model is an appropriate for optoelectronic devices. In addition, the characterizations, analysis and optical studies recommended CdS nanostructures for photovoltaic and optoelectronic applications.

Acknowledgments

Y.A. would like to acknowledge University Malaysia Perlis for grants Nos. 9007-00111 & 9007-00185 and TWAS-Italy for the full support of his visit to JUST-Jordan under TWAS-UNESCO Associateship. A.H.R. would like to acknowledge the CENTEM project, reg. no. CZ.1.05/2.1.00/03.0088, cofunded by the ERDF as part of the Ministry of Education, Youth and Sports OP RDI Programme and, in the follow-up sustainability stage, supported through CENTEM PLUS (LO1402) by financial means from the Ministry of Education, Youth and Sports under the "National Sustainability Programme I". Also would like to acknowledge MetaCentrum (LM2010005) and CERIT-SC (CZ.1.05/3.2.00/08.0144) infrastructures.

References

[1] S.J. Ikhmayies, R.N. Ahmad-Bitar, Characterization of the SnO2:F/CdS:In structures prepared by the spray pyrolysis technique, Sol. Energy Mater. Sol. Cells 94 (2010) 878–883.
[2] A.I. Oliva, P. Quintana, D.H. Aguilar, W. Cauich, M. Ortega, Y. Matsumotoa, Hexagonal phase of CdS thin films obtained by oscillating chemical bath, J. Electrochem. Soc. 155 (2008) D158–D162.
[3] Dumbrava, C. Badea, G. Prodan, V. Ciupina, Synthesis and characterization of cadmium sulphide obtained at room temperature, Chalcogenide Lett. 7 (2010) 111–118.
[4] C.H. Huang, Sheng S. Li, W.N. Shafarman, C.-H. Chang, E.S. Lambers, L. Rieth, J.W. Johnson, S. Kim, B.J. Stanbery, T.J. Anderson, P.H. Holloway, Study of Cd-free buffer layers using $In_x(OH,S)_y$ on CIGS solar cells, Sol. Energy Mater. Sol. Cells 69 (2001) 131–137.
[5] A. Kylner, A. Rockett, L. Stolt, Oxygen in solution-grown CdS films for thin film solar cells, Solid State Phenom. 51–52 (1996) 533–540.
[6] D.W. Niles, G. Herdt, M. Al-Jassim, An X-ray photoelectron spectroscopy investigation of O impurity chemistry in CdS thin films grown by chemical bath deposition, J. Appl. Phys. 81 (1997) 1978–1984.
[7] R. Seoudi, A.A. Shabaka, M. Kamal, E.M. Abdelrazek, Dependence of spectroscopic and electrical properties on the size of cadmium sulfide nanoparticles, Physica E 45 (2012) 47–55.
[8] Y. Al-Douri, H. Baaziz, Z. Charifi, R. Khenata, U. Hashim, M. Al-Jassim, Further optical properties of CdX (X = S, Te) compounds under quantum dot diameter effect: ab initio method, Renew. Energy 45 (2012) 232–236.
[9] Y. Al-Douri, R. Khenata, A.H. Reshak, Investigated optical studies of Si quantum dot, Sol. Energy 85 (2011) 2283–2287.
[10] R.A. Joshi, V.S. Taur, A.V. Ghule, R. Sharma, Stoichiometry controlled conversion efficiency in nanostructured heterojunction solar cell of $CdS/CuInS_XSe_{2-X}$ grown by chemical ion exchange method at room temperature, Sol. Energy 85 (2011) 1316–1321.
[11] K.W. Böer, Energy Convers. Manag. 52 (2011) 426–430.
[12] A.S.Z. Lahewil, Y. Al-Douri, U. Hashim, N.M. Ahmed, Structural and optical investigations of cadmium sulfide nanostructures for optoelectronic applications, Sol. Energy 86 (2012) 3234–3240.
[13] A.M. Sherry, M. Kumar, Analysis of thermal expansion for alkali halide crystals using the isobaric equation of state, J. Phys. Chem. Solids 52 (1991) 1145–1148.
[14] J.L. Tallon, The thermodynamics of elastic deformation-I: equation of state for solids, J. Phys. Chem. Solids 41 (1980) 837–850.
[15] Y. Al-Douri, H. Abid, H. Aourag, Correlation between the bulk modulus and the charge density in semiconductors, Physica B 305 (2001) 186–190.
[16] Y. Al-Douri, H. Abid, H. Aourag, Calculation of bulk moduli of semiconductor compounds, Physica B 322 (2002) 179–182.
[17] Y. Al-Douri, The pressure effect of the bulk modulus seen by the charge density in CdX compounds, Mater. Chem. Phys. 78 (2003) 625–629.
[18] Y. Al-Douri, H. Abid, H. Aourag, Correlation between the bulk modulus and the transition pressure in semiconductors, Mater. Lett. 59 (2005) 2032–2034.
[19] J.C. Phillips, Bonds and Bands in Semiconductors, Academic Press, San Diego, 1973.
[20] W.A. Harison, Electronic Structure and the Properties of Solids, General Publishing Company, Toronto, 1989.
[21] M.L. Cohen, Handbook of Materials Modeling, Phys. Rev. B 32 (1985) 7988–7991.
[22] P.K. Lam, M.L. Cohen, G. Martinez, Analytic relation between bulk moduli and lattice constants, Phys. Rev. B 35 (1987) 9190–9194.
[23] Y. Al-Douri, H. Abid, H. Aourag, Empirical formula relating the bulk modulus to the lattice constant in tetrahedral semiconductors, Mater. Chem. Phys. 87 (2004) 14–17.
[24] J.J. Tan, Y. Li, G.F. Ji, High-pressure phase transitions and thermodynamic behaviors of cadmium sulfide, Acta Phys. Pol. A 120 (2011) 501–506.
[25] H. Metin, S. Erat, S. Durmus, M. Ari, Annealing effect on CdS/SnO_2 films grown by chemical bath deposition, Appl. Surf. Sci. 256 (2010) 5076–5081.
[26] D.H. Rose, D.H. Levi, R.J. Matson, D.S. Albin, R.G. Dhere, P. Sheldon, The Role of Oxygen in CdS/CdTe Solar Cells Deposited by Close-Spaced Sublimation, 1996, pp. 777–780.
[27] R. Castro-Rodriguez, J. Mendez-Gamboa, I. Perez-Quintana, R. Medina-Ezquivel, CdS thin films growth by fast evaporation with substrate rotation, Appl. Surf. Sci. 257 (2011) 9480–9484.
[28] Y. Shim, M.E. Mills, V. Borovikov, J.G. Amar, Effects of substrate rotation in oblique incidence metal (100) epitaxial growth, Phys. Rev. E 79 (2009) 051604–051606.
[29] M. Elango, K. Gopalakrishnan, S. Vairam, M. Thamilselvan, Structural, optical and magnetic studies on non-aqueous synthesized CdS:Mn nanomaterials, J. Alloys Compd. 538 (2012) 48–55.

[30] K. Ravichandran, P. Philominathan, Investigations on microstructural and optical properties of CdS films fabricated by a low-cost, simplified spray technique using perfume atomizer for solar cell applications, Sol. Energy 82 (2008) 1062–1066.
[31] S. Thangavel, S. Ganesan, K. Saravanan, Annealing effect on cadmium in situ doping of chemical bath deposited PbS thin films, Thin Solid Films 520 (2012) 5206–5210.
[32] M.A. Mahdi, S.J. Kasem, J.J. Hassen, A.A. Swadi, S.K.J. Al-Ani, Structural and optical properties of chemical deposition CdS thin films, Nanoelectron. Mater. 2 (2009) 163–172.
[33] Y. Al-Douri, Y.P. Feng, A.C.H. Huan, Optical investigations using ultra-soft pseudopotential calculations of $Si_{0.5}Ge_{0.5}$ alloy, Solid State Commun. 148 (2008) 521–524.
[34] Y. Al-Douri, A.H. Reshak, H. Baaziz, Z. Charifi, R. Khenata, S. Ahmad, U. Hashim, An ab initio study of the electronic structure and optical properties of $CdS_{1-x}Te_x$ alloys, Sol. Energy 84 (2010) 1979–1984.
[35] R.C. Weast, Handbook of Chemistry and Physics, 53rd ed., CRC Press, USA, 1972.
[36] N.M. Ravindra, S. Auluck, V.K. Srivastava, On the Penn gap in semiconductors, Phys. State Solid B 93 (1979) k155–k160.
[37] P.J.L. Herve, L.K.J. Vandamme, Empirical temperature dependence of the refractive index of semiconductors, J. Appl. Phys. 77 (1995) 5476–5477.
[38] D.K. Ghosh, L.K. Samanta, G.C. Bhar, A simple model for evaluation of refractive indices of some binary and ternary mixed crystals, Infrared Phys. 24 (1984) 34–47.
[39] D.R. Penn, Wave-number-dependent dielectric function of semiconductors, Phys. Rev. 128 (1962) 2093–2097.
[40] J.A. Van Vechten, Quantum dielectric theory of electronegativity in covalent systems. I. Electronic dielectric constant, Phys. Rev. 182 (1969) 891–905.
[41] G.A. Samara, Temperature and pressure dependences of the dielectric constants of semiconductors, Phys. Rev. B 27 (1983) 3494–3505.